In-situ X-ray Observation of Molten Pool Depth during Laser Micro Welding

Tomonori YAMADA[*1], Takahisa SHOBU[*2], Akihiko NISHIMURA[*1], Yukihiro YONEMOTO[*1], Susumu YAMASHITA[*1] and Toshiharu MURAMATSU[*1]

[*1] *Japan Atomic Energy Agency, 65-20 Kizaki, Tsuruga, Fukui 914-8585, Japan*
E-mail: yamada.tomonori41@jaea.go.jp
[*2] *Japan Atomic Energy Agency, 1-1-1 Kouto Sayo-cho, Sayo-gun, Hyogo 679-5148, Japan*

To clarify phenomena which cause strength decrease in the molten pool during laser welding processes, we have carried out X-ray imaging of inside materials using intense synchrotron radiation during laser welding. An air-cooled continuous wave fiber laser was used for welding. When the laser beam was irradiated on sample materials, molten pool shape were successfully observed using an X-ray absorption contrast technique. Moreover, bubbles in molten pool and cracks in weld metal were clearly observed. Butt welding for heat exchanger tubes was demonstrated by a specially designed probing system. The probing system consisted on a composite-type optical fiber, a laser processing head, air-cooled fiber laser and so on. Here, the surface of the weld bead was observed by fiber scope images. In such a repair welding, the observation of the inside material by X-ray imaging is very effective because it can inform us how the weld depth could grow and why the weld defect would be born.

DOI:10.2961/jlmn.2012.03.0002

Keywords: Intense X-ray beam, Laser welding, Molten pool, X-ray imaging, Bubbles, Cracks

1. Introduction

Some of Japan's oldest nuclear power plants are now entering their 40th year. To extend their designed lifespan up, in-situ flaw sizing and repairs are needed [1]. Careful attention should be required for material degradation caused by water corrosion and radiation damage. For the repairing technology, laser welding shows important advantages compared with other welding techniques, as low heat input, high localization ability, the high welding speed, the high flexibility, the high weld quality and the high production rate. Moreover, the use of fiber laser surely improves processing accuracy. The new probing system was recently developed to treat micro cracks at the welded section of heat exchanger tubes, where a fiber laser beam passed through a composite-type optical fiber scope. Molten pool diameter by laser welding gradually expanded more than the width of the micro crack's crevice caused by stress corrosion cracking [2].

For the standardization of the laser repairing technology, physical understanding of the mechanisms with higher accuracy and higher resolution for the complex phenomena is extremely important. In our laboratory, SPLICE (residual Stress control using Phenomenological modeling for Laser welding repair process In Computational Environment) code [3] is developed to simulate the laser welding process and evaluate the residual stress in the welded material. At the present time, we have preliminary studied the welding process from viewpoint of experiment and numerical simulation.

SPring-8 (Super Photon ring-8 GeV) is a large synchrotron radiation facility which delivers the most powerful synchrotron radiation currently available. For example, X-ray imaging is utilized for the visualization of internal structures of objects in a large number of fields such as materials science, condensed matter physics, etc.. In welding process, in-situ observation of the solidification process by X-ray imaging [4] and the phase transformation have been carried out using time-resolved X-ray diffraction system [5]. In our project, a molten pool during laser welding is observed [6]. A direct observation of the molten pool during laser welding is applicable to understand the melting/ solidification processes. Moreover, a three dimensional residual strain is measured experimentally after laser irradiation [7]. The three dimensional measurement of the residual stress is key technology for high accurate evaluation of our SPLICE code in the future.

In the present work, we have carried out in-situ X-ray observation of inside materials during laser butt welding using intense synchrotron radiation for repairing the micro crack's crevice as a practical demonstration and causes of strength decrease were observed during welding processes.

2. Experimental procedures

2.1 In-situ X-ray observation

The studied materials were SUS316 austenitic stainless steel having the dimensions of 20 mm length × 5mm width × 5mm thickness. The chemical compositions of these materials are given in Table 1. Tungsten particles were used as a motion or boundary tracer in a molten pool.

In-situ X-ray observation was carried at the undulator beam line (BL22XU) in SPring-8. In order to clearly observe the tungsten particles, the energy of X-rays monochromatized by two Si 111 crystals selected 70.3 keV which was a little high energy of the X-ray K-absorption edge of tungsten. The sizes of X-ray beam were 2.5 mm × 4.3 mm. Specimens were set on the linear move stage. The schematic illustration of in-situ observation during butt welding is shown in Fig.1. When the laser beam was irradi-

ated on the interface of the two samples, laser welding processes were successfully observed using X-ray absorption contrast method. The charge coupled device (CCD) camera made of Hamamatsu photonics K.K. was used to obtain images of those processes, and was set up at a position away from specimens by 120cm. Exposure time and time resolution of that CCD camera in this study were 32 ms and 111ms, respectively.

A continuous wave ytterbium fiber laser (IPG YLR-300-AC) was used for welding. The beam quality (M^2) was 1.03 and the emission wavelength is 1070 nm. Laser beam was focused to the specimen surface from the distance of 205 mm. The spot diameter was 1.074 mm and the power density 39 kW/cm^2. Table 2 shows the experimental conditions in the welding process.

After welding, the photograph of weld bead was taken by an optical microscope (OM). The specimens for metallography were obtained from the transverse direction of weld, followed by mechanical polishing by standard technique and etched.

Table 1 Chemical composition of SUS316

C	Si	Mn	P	S	Ni	Cr	Mo
0.05	0.3	1.32	0.034	0.026	10.27	16.9	2

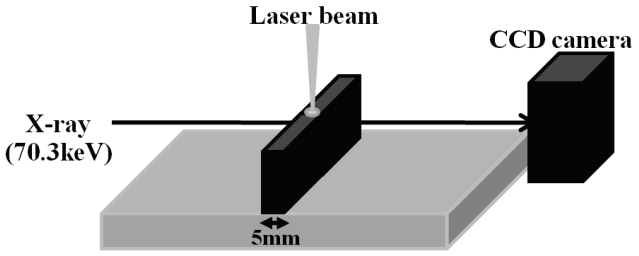

(a) Spot welding

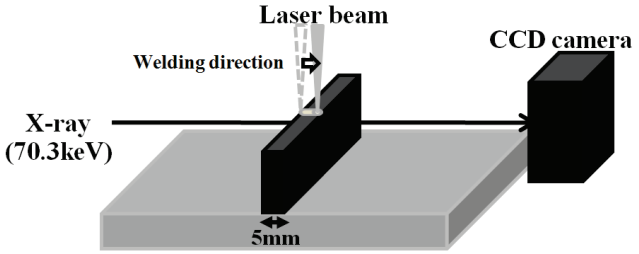

(b) Bead-on-plate welding

Figure 1 Schematic illustration of in-situ observation during butt weld.

Table 2 Experimental condition

Sample material	Stainless steel		
Energy of X-ray	70.3 keV		
Focal length	205 mm		
Wavelength	1070 nm		
Focal position	0 mm		
Laser power	200W	300W	330W
Welding speed	1 mm/s		
Spot welding		20 s	20 s

2.2 Laser welding for a heat exchanger tube

Laser welding with an optical fiber is promising to maintain complex piping systems. A prototype probing system was developed for the maintenance next generation Fast Breeder Reactors [2]. The specially designed probing head was inserted into the heat exchanger tube. The tube inner wall was inspected to find cracks by a composite-type optical which delivered laser beam. Laser welding is effective for repairing the deep cracks. By applying this probing system to aging Light Water Reactors, significant cost and time in plant operation could be saved. Thus, the following experiment is the first step of the practical demonstration of the bead-on-plate welding shown in Fig. 1 (b).

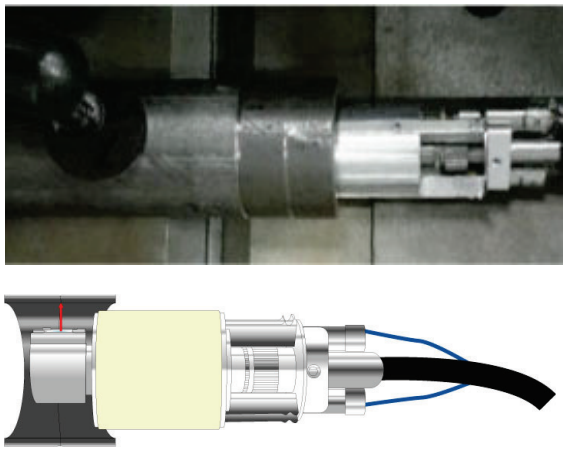

Figure 2 Laser welding for a heat exchanger tube
(a) Test tubes and laser processing head (upper)
(b) Cut view of the laser welding experiment (lower)

Figure 2 (a) shows the photograph of experimental set-up of laser welding for a heat exchanger tube. Here, the laser processing head was inspecting the inner wall of the test pieces of 1-inch diameter tube. Figure 2 (b) shows the cut view of the laser processing head at the inlet of the heat exchanger tube. A pair of short tubes of STKM13A was used. Table 3 shows the chemical composition. These short tubes had 10 mm length with 23 mm diameter and 4.5 mm thickness. These were contacted to be processed as butt welding. Rotational motion of a 55 degree tilted mirror inside the laser processing head successfully scanned a laser spot along the interface of the tubes. Scanning speed of the laser spot was tested from 1.4 mm/s to 4.2 mm/s. Air velocity of 20 m/s during welding was constantly maintained.

Table 3 Chemical composition of STKM13A

C	Si	Mn	P	S
0.16	0.20	0.48	0.017	0.007

3. Results and Discussion

3.1 Evaluation of X-ray imaging contrast

Figure 3 shows an image of a molten pool during spot welding and X-ray intensity profiles. The fiber laser power was 330 W. It is known that density of liquid phase of pure iron is 7015 kg/m^3 at 1809 K and the density of solid phase is 7874 kg/m^3 at room temperature [8]. Here, the 11 % difference in density made it possible to observe the fusion line by 70.3 keV synchrotrons X-ray. Moreover, the contrast difference can be confirmed in molten pool. The black

contrast was observed in center of molten pool and white contrast was observed in interfacial neighborhood. To investigate this contrast difference, X-ray intensity was measured at broken line as shown in Fig. 3 (b). The X-ray intensity was increased inside of the fusion line and was decreased outside of the fusion line, as shown Fig. 3 (c) (circle). This edge enhancement was a feature of refraction contrast. In absorption contrast, the contrast results from variation in X-ray absorption arising from density differences and from variation in the thickness and composition of the sample materials. In refraction contrast, shape of sample materials and boundary of the internal structure are enhanced. Therefore, the fusion line was enhanced by refraction contrast.

Figure 4 shows a result of optical microscope observation for the sample material after welding. In this figure, dendrites are observed and dendrites have grown from fusion line to inside molten pool. It is known that the dendrites arm spacing was very important for a control of microstructural feature. In our X-ray imaging, the shape of dendrites was not observed because the thicknesses of sample materials were large.

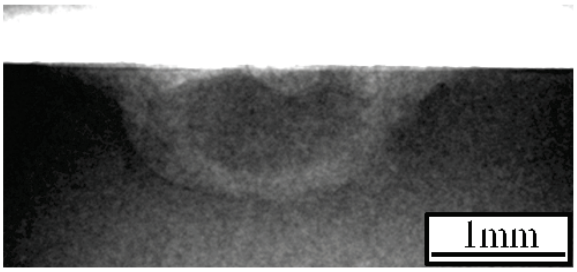

(a) X-ray imaging

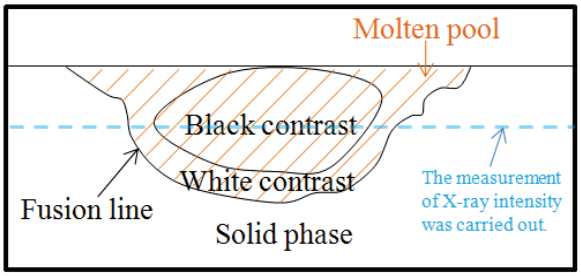

(b) Schematic illustration of X-ray imaging

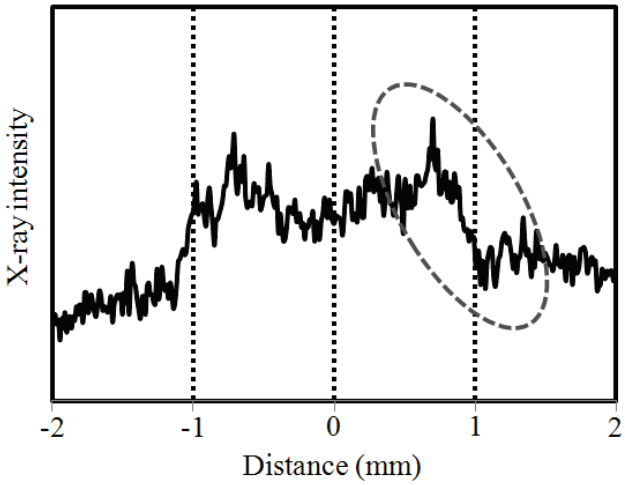

(c) X-ray intensity profiles

Figure 3 Observed images of molten pool by X-ray contrast

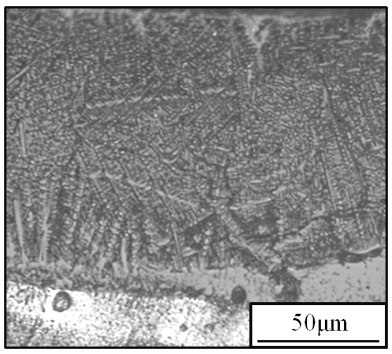

Figure 4 Microstructure of stainless steels

3.2 Phenomena of molten pool during laser welding

Figure 5 shows an image of a molten pool during butt welding (spot welding) by the X-ray CCD camera. The crevice of the two samples shows a well-lighted white line. The fiber laser power was 300 W. At 300 ms just after the laser irradiation, a molten zone with 0.2 mm depth was observed as gray shadow on the top of the crevice. The laser irradiation time of 7 second was necessary to get the molten pool with 0.85 mm depth. As a result, we were able to confirm the growth of the molten pool depth during the laser welding process. Figure 6 shows growth of the molten pool depth. We were able to confirm the growth of the molten pool depth during laser welding process. The molten pool depth was about 1.2 mm at 20 second.

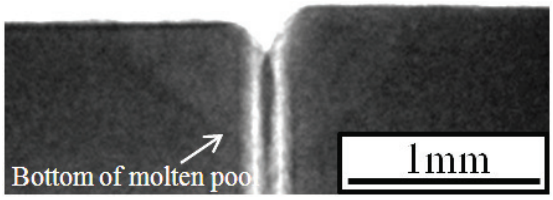

Figure 5 Observed images of molten pool by X-ray absorption contrast in continuous laser welding process.

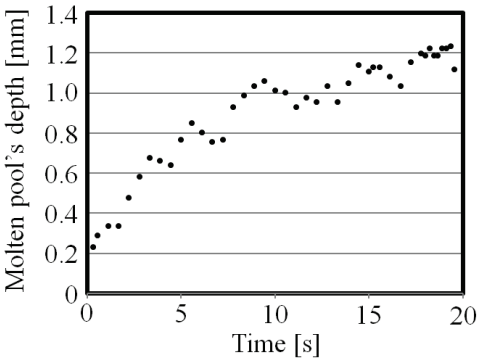

Figure 6 Growth of molten pool depth

When it keeps irradiating the laser beam to the sample material, molten pool becomes unstable and bubbles were observed. Figure 7 (a) shows bubbles in the molten pool. Theses bubbles were generated from the neighbor of the fusion line. In the case of high-power laser welding, the stability of the keyhole is important because bubbles are generated at the keyhole tip [9]. However, in our study, molten pool was not a keyhole type but a heat conduction type. It could be thought that the cause of these bubbles was dissolved gas inside materials. Figure 7 (b) and (c)

show the X-ray image after laser irradiation and microstructure on cross-section. In the X-ray image, bubbles which were observed during laser welding remain after solidification. In OM observation on cross-section, a lot of porosities were found. These porosities corresponded to bubbles which were observed by X-ray absorption contrasts because it existed in the same place. As a result, the prolonged laser irradiations to the sample materials cause the porosity. Hence, by shortening the laser irradiation time, the porosity could be reduced.

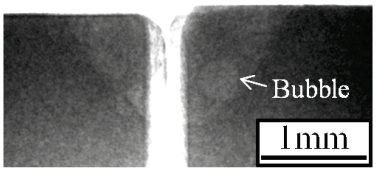

(a)X-ray image during laser welding

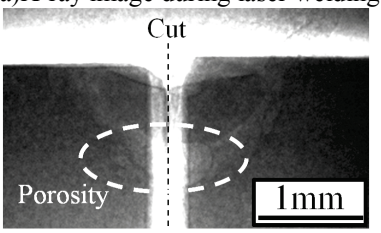

(b)X-ray image after laser irradiation

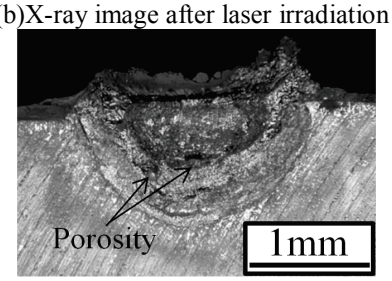

(c) Microstructure on cross-sectional (right side of (b))

Figure7 X-ray imaging during/after laser welding and Microstructure in as welded.

Figure 8 shows the X-ray image of butt welding (Bead-on-plate welding). The fiber laser power was 200 W and welding speed was 1mm/s. The molten pool depth was about 0.3 mm and it was steady during welding. The bubble was observed during laser welding. Moreover, white line was observed in molten pool. Figure 9 (a) shows the X-ray image after laser welding. The white line was grown from bottom of weld metal to the surface after laser irradiation. Figure 9 (b) shows the overview of weld bead. Oxidized scales were observed on the weld bead surface because the welding was performed under air environment. Moreover, the crack was observed at the center of weld bead. Thus, the white line was crack, in Fig. 9 (a). Therefore, in our observation, the internal crack could be found during laser welding.

As stated above, X-rays imaging can specify the occurrence time and the generation point of the defect. In an on-site maintenance process, it is very difficult to observe the behavior of the inside material from the surface observation. Therefore, it is useful to understand a relationship between inner behavior of materials and a laser condition from a material surface. In the next section, the laser butt welding in the 1-inch tube is demonstrated and discussed on the basis of the results in this section.

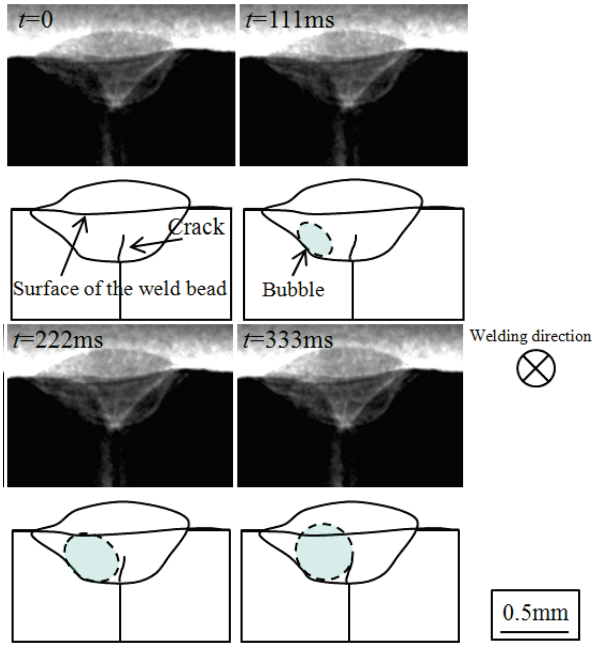

Figure 8 X-ray imaging during bead-on-plate welding. (Welding speed 1mm/s, laser power 200W)

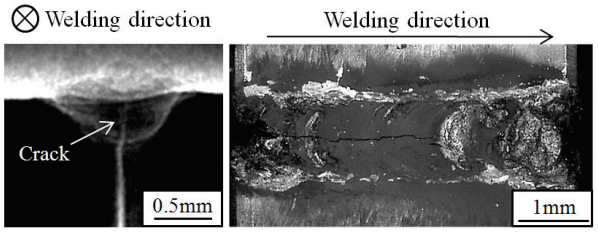

(a) X-ray image (b) Overview of weld bead

Figure 9 X-ray image and overview after laser welding.

3.3 Laser welding maintenance for heat changer units

Laser welding maintenance by a composite-type optical fiber is expected for heat exchanger units. Careful attention should be paid for corrosion and cracking. Especially in case of very high temperature or corrosive fluid, even a small crack is surely connected directly with a big accident. When the flow vibrates, it is more troublesome. The following is observation of laser butt welding by the prototype probing system.

Figure 10 shows the example of the butt welding experimental results. The laser spot scanning speed was 1.4 mm/s and laser output power was 330 W. These images were taken by the composite-type optical fiber scope just after the butt welding. Figure 10 (a) shows the position of starting position of the laser welding. A circle at the center of the photograph is a part of the fiber that transmits high energy laser beam. The part from the center to the left diagonal direction shows the contacted interface of the short tubes without laser irradiation. As for the right diagonal direction, the welding bead was clearly formed. The length of the welding bead was 14 mm and the scanning time was 10 seconds that corresponded with 70 degree. During observation, these inner wall images rotated in keeping with scanning. Here the welding bead has constant width of 1.5 mm and smooth welding surface shown in both Fig. 10 (b) and Fig.10 (c). At the end of the welding bead, a molten pool of 2 mm diameter was formed in Fig. 10 (d). Inside

materials are predictable from the result of X-ray imaging. For example, comparing the in-situ X-ray absorption and the microscopic observation, the molten pool depth of around more than 0.3 mm could be expected. Moreover, it is expected that short laser irradiation time could reduce the porosity of the molten pool.

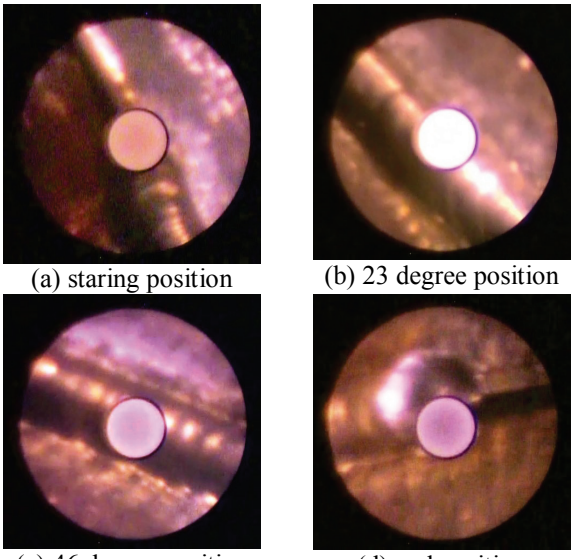

(a) staring position (b) 23 degree position

(c) 46 degree position (d) end position

Figure 10 the example of the butt welding
These views are taken from the inside of 1-inch tube by a composite-type optical fiber scope.

The molten pool depth of 0.3 mm would be useful to suppress SCC although it must be too thin to repair a deep crack completely. For example, in the case of SCC in Boiling Water Reactor in Japan, it was investigated that intergranular SCC observed in almost whole fracture surface were developed from the initiation of transgranular SCC [10]. Hardening layers from the surface to the depth of a few hundred μm could cause the TGSCC. So it is expected that the TGSCC surface melts, solidifies, and becomes a lid. This lid obstructs the inside infiltration of water newly. If water dissolving oxygen is not infiltrated, the growth of the crack is controlled.

Multinational design evaluation programme and its impact on the regulation for severe accidents have been reported [11]. Laser micro welding could play important role in mitigation for the severe accidents. For the severe accident of heat exchanger units of aging nuclear power plants, the Emergency Core Cooling System (ECCS) was activated at the first time in Japan. It was on Feb. 1991 that leakage of primary coolant at Mihama Pressurized Water Reactor Unit 2 due to failure of steam generator tube occurred. Leakage of radioactive 55 tons of primary coolant immediately caused the reactor shutdown. After the accident, fiber scope inspection was carried out to find the failure of a heat exchanger tube. The facture surface of the failed tube was examined by scanning electron microscope observation, which clarified that this accident was caused by fatigue fracture. It was subjected to flow-induced vibration and damage by frequent fretting. Laser micro welding by the prototype probing system is expected to repair the fatigue in the future, which will reduce the risk of severe accidents.

4. Conclusions

Micro spot welding by a fiber laser will be used in order to repair cracks on welded sections of aging nuclear power stations. In the present study, in-situ observation of molten pool during fiber laser butt welding was carried out using an intense synchrotron radiation for repairing the micro crack's crevice as a practical demonstration and causes of strength decrease were observed during welding processes.

The depth of molten pool grew up to 1.2 mm at 20 seconds using 300 W of laser power. Therefore, we may repair the micro crack using this laser if the crack depth is less than 1mm. However, the prolonged laser irradiation to the sample materials causes porosity.

In-situ observation of inside materials during fiber laser welding provides a useful knowledge of repair welding because bubbles and cracks which cause the poor weld was clearly observed in non-destructive. This is very effective for control of weld defect and investigation of the mechanisms.

Acknowledgments

We are grateful to Dr. H. Daido of JAEA for his useful suggestions and Mr. Y. Takenaka for his technical assistance of laser welding. We also appreciate Prof. S. Katayama, Prof. Y. Komizo and Dr. H. Terasaki of Joining and Welding Research Institute of Osaka University. We also thank the assistance of Dr. K. Kajiwara of Japan Synchrotron Radiation Research Institute. The synchrotron radiation experiments were performed with the approval of the JASRI (proposal no. 2010B3721).

References

[1] Y. Yamashita: J. Nucl. Sci. Tech., 38, (2001) 887.
[2] A. Nishimura, T. Shobu, K. Oka, T. Yamaguchi, Y. Shimada, et al.: Journal of Japan Laser Processing Society, 17, 4 (2010) 207.
[3] S. Yamashita, Y. Yonemoto, T. Yamada, T. Kunugi and T. Muramatsu: The Visual-JW 2010 Symposium, 1, JWP-15 (2010).
[4] H. Yasuda, T. Nagira, M. Yoshiya, M. Uesugi, N. Nakatsuka and A. Sugiyama: SPring-8 Information, 16, 1 (2011) 10.
[5] Y. Komizo, H. Terasaki, M. Yonemura and T. Osuki: Q. J. Jpn. Weld. Soc., 24, 1 (2006) 57.
[6] T. Yamada, T. Shobu, Y. Yonemoto, S. Yamashita, A. Nishimura and T. Muramatsu: Proc. of ICONE19, Chiba, (2011).
[7] T. Shobu, et al.: MECA SENS V/QuBS2009 Laser welding and forming at Mito OS-59 (2009).
[8] I. Ohnaka: "An introduction to computerized heat transfer and solidification analysis", (Maruzen Co., Ltd., Tokyo, 1985).
[9] Y. Kawahito, M. Mizutani and S. Katayama: Q. J. Jpn. Weld. Soc., 26, 3 (2008) 203.
[10] T. Tsukada, et al., JAERI-Tech 2004-044, (2004).
[11] Y. Tsujikura, et al., Journal of the Atomic Energy Society of Japan, 53, 4 (2011) 255.

(Received: June 07, 2011, Accepted: May 31, 2012)